Tetrahedron 64 (2008) 7437–7443

Contents lists available at ScienceDirect

Tetrahedron

journal homepage: www.elsevier.com/locate/tet

Mechanistic insights into the transmetalation step of a Suzuki–Miyaura reaction of 2(4)-bromopyridines: characterization of an intermediate

Cristina Sicre [a], Ataualpa A.C. Braga [b], Feliu Maseras [b,c], M. Magdalena Cid [a,*]

[a] Departamento de Química Orgánica, Facultade de Química, Universidade de Vigo, Campus Lagoas-Marcosende, 36310 Vigo, Spain
[b] Institute of Chemical Research of Catalonia (ICIQ), Av. Països Catalans, 16, 43007 Tarragona, Spain
[c] Departament de Química, Universitat Autònoma de Barcelona, 08193 Bellaterra, Spain

ARTICLE INFO

Article history:
Received 18 January 2008
Received in revised form 6 May 2008
Accepted 7 May 2008
Available online 10 May 2008

Keywords:
2-Bromopyridines
Suzuki reaction mechanism
DFT calculations
Palladium catalysis

ABSTRACT

The mechanistic study of the palladium-catalyzed Suzuki–Miyaura cross-coupling between bromophenylpyridine compounds and phenylboronic acid led to the NMR identification of a transient intermediate in the transmetalation step. This species was identified by DFT calculations as a [Pd{Ph-B(OH)$_3^-$}{C_5H_2RN}(PR_3)$_2$] complex, containing a boronate ligand coordinated through an oxygen group to the metal center. The fitting of this intermediate within recent mechanistic proposals on the mechanism of transmetalation is discussed.

1. Introduction

Palladium-catalyzed reactions are particularly effective for the construction of unsymmetrical biaryls and have revolutionized synthetic routes to arylated heterocyclic compounds,[1] structural motifs in many natural products and in pharmaceutical agents.[2] The palladium-catalyzed cross-coupling process between an organoboronic acid and an organic halide, known as the Suzuki–Miyaura reaction,[3] has become one of the most reliable and widely applied palladium-catalyzed cross-coupling reactions in total synthesis.[4]

The coupling of organoboranes is believed to proceed through a catalytic cycle involving three basic steps: the oxidative addition of a carbon electrophile to a coordinatively unsaturated PdL or PdL_2, the transmetalation of a nucleophilic carbon from boron to $RPdXL_2$ with the aid of bases, and the rapid reductive elimination of the cross-coupling product with regeneration of the PdL or PdL_2 catalyst (Fig. 1). The catalytic cycle depicted in Figure 1 only schematically represents what is quite clearly a highly complex process.[5] The oxidative addition and reductive elimination steps have been the subject of several experimental and theoretical studies.[6] In contrast, detailed reaction mechanisms of transmetalation still remain unclarified in many cases, although they are closely related to a number of synthetic reactions catalyzed by transition metal complexes.[7] The experimental difficulty in the characterization of possible intermediates in transmetalation[8] has led to a substantial role for computational chemistry in the definition of the detailed mechanism for the reaction.[9,10] Theoretical studies indicate that transmetalation is a complex process going through several intermediates. Nevertheless, it is known that the initial step is the attack of a base on the organoboronic acid, which then reacts with the palladium species in an organoboronate form. It would be certainly desirable to find experimental support for this mechanistic hypothesis through the characterization of reaction intermediates, but this is a difficult task because of their transient nature.

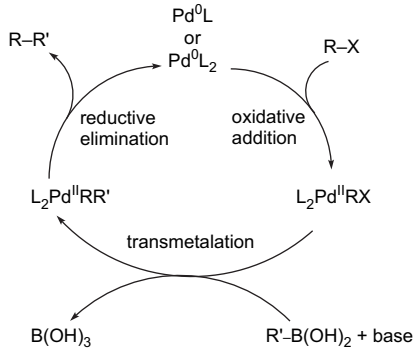

Figure 1. Suzuki–Miyaura catalytic cycle.

* Corresponding author. Tel.: +34 986813563; fax: +34 986812262.
E-mail address: mcid@uvigo.es (M.M. Cid).

0040-4020/$ – see front matter © 2008 Elsevier Ltd. All rights reserved.
doi:10.1016/j.tet.2008.05.018

Due to the abundance of halopyridines, Suzuki–Miyaura reactions in which they serve as electrophiles have been used to synthesize a plethora of arylpyridines and heteroarylpyridines. Our interest in the preparation of complex pyridine-containing molecules[11] led us to study the mechanism of cross-coupling processes of bromide-substituted pyridyl compounds, in particular the Suzuki–Miyaura reaction. Recently, we have described regioselective Suzuki–Miyaura cross-coupling reactions between 2,4-dibromopyridine and several aryl boronic acids that furnished, under $Pd(PPh_3)_4$ catalysis, mainly 2-aryl-4-bromo-pyridines due to the higher electrophilic character of the C–Br bond at position 2 of the pyridine ring and to the absence of double oxidative addition products. We have also ascribed the observed low TON to the formation of a dinuclear palladium complex from the mononuclear σ-alkenyl palladium complex.[12]

The need to unfold the mechanism of the Suzuki–Miyaura cross-coupling reaction at both reactive positions of 2,4-dibromopyridine prompted us to study such reaction of 2- and 4-bromopyridine in order to mimic independently the reactive centers of 2,4-dibromopyridine. Here, we report a mechanistic study of the transmetalation step of the Suzuki–Miyaura reaction between the 2(4)-bromo-4(2)phenylpyridines **1a** and **1b** and phenylboronic acid (**2**) (Scheme 1) in the presence of $Pd(PPh_3)_4$ and aq K_2CO_3 to produce 2,4-biphenylpyridine (**3**) monitored by ^1H and ^{31}P NMR spectroscopies along with a theoretical study of the transmetalation step.

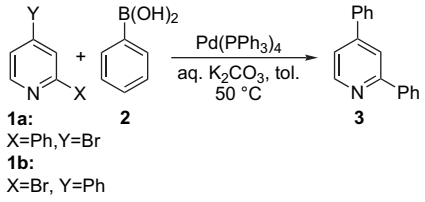

Scheme 1. Suzuki–Miyaura cross-coupling reaction.

2. Results and discussion

2.1. Experimental study

To investigate the mechanism of the Suzuki–Miyaura reaction depicted in Scheme 1, we have chosen $Pd(PPh_3)_4$ as the catalyst, because it had rendered the best results regarding conversion and selectivity, K_2CO_3 and toluene as base and solvent, respectively. The reactions have been carried out at 50 °C in order to be able to compare the reactivity of pyridines **1a** and **1b**, since the oxidative addition of the former to $Pd(PPh_3)_4$ is very slow at temperatures below 50 °C.

In order to facilitate the study of the subsequent transmetalation step, the oxidative addition complexes of the reaction of bromophenylpyridines **1a** and **1b** with $Pd(PPh_3)_4$ were characterized first.[13] Thus, the reaction between 4-bromo-2-phenylpyridine (**1a**) and 100 mol % of $Pd(PPh_3)_4$ at 50 °C in toluene afforded *trans*-[$PdBr\{C_5H_3N(2\text{-}C_6H_5)\text{-}C^4\}(PPh_3)_2$] complex **4a** in 73% yield. The presence of a singlet in the ^{31}P NMR spectrum (24.13 ppm, CD_2Cl_2) confirmed a trans disposition of the ligands. Its ^1H NMR shows the pyridine proton shifts upfield compared to the bromopyridine **1a** signals due to an anisotropic shielding effect of the triphenylphosphine ligand as well as by back donation from the palladium to the pyridine ring. When the reaction was run with pyridine **1b** and 100 mol % of $Pd(PPh_3)_4$ at 25 °C in toluene, a mixture of the mononuclear complex **4b**, *trans*-[$PdBr\{C_5H_3N(4\text{-}C_6H_5)\text{-}C^2\}(PPh_3)_2$], and the dinuclear complex **4b-D**, *trans*-(*P,N*)-[$PdBr\{\mu\text{-}C_5H_3(4\text{-}C_6H_5)\text{-}C^2,N\}(PPh_3)]_2$, was obtained in 30% yield.[14] The ^{31}P NMR signals appeared at 22.12 and 30.32 ppm, respectively (Scheme 2).[15]

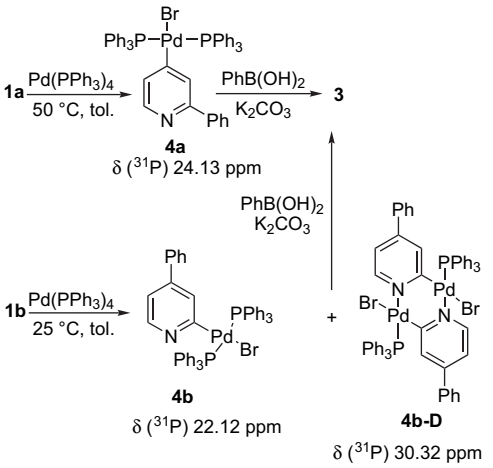

Scheme 2. Stepwise Suzuki–Miyaura cross-coupling reaction of bromopyridines **1a** and **1b**.

The structure of complex **4b-D** was confirmed by X-ray analysis, which showed a boat conformation for the six-membered ring containing both Pd and N with a dihedral angle of 89.6° between both pyridine ring-containing planes. Each palladium atom exhibits a square-planar geometry with bromide and phosphine trans to carbon and nitrogen, respectively.[16]

When the oxidative addition of compound **1a** to $Pd(PPh_3)_4$ was conducted in an NMR sample tube in deuterated toluene at 50 °C in an NMR spectrometer probe, two signals were observed in the ^{31}P NMR spectrum: the one corresponding to complex **4a** (24.13 ppm) and another at 24.41 ppm due to the presence of traces of triphenylphosphine oxide. There was also a very broad signal (12–15 ppm), whose chemical shift varied depending on the amount of ligand and which is a consequence of fast equilibria between free and coordinated phosphine.[17]

However, in the case of compound **1b**, at short reaction times, only the signal at 22.12 ppm was observed but as the reaction moved forward, the signal due to the dimer complex **4b-D** at 30.22 ppm became more significant. The oxidative addition at 50 °C at position 2 of the pyridine ring turned out to be much faster than that at position 4 (10 min vs 10 h).

With the oxidative addition complexes in hand, we proceeded to study the transmetalation step of the catalytic cycle of the Suzuki–Miyaura cross-coupling by means of ^1H and ^{31}P NMR spectroscopies. Thus, the cross-coupling reaction of **1a** with phenylboronic acid in the presence of 100 mol % of $Pd(PPh_3)_4$ at 50 °C was complete in 14 h, being complex **4a** the only observable soluble species in the transmetalation reaction. The other signals in the spectrum were assigned to: (a) Ph_3PO in the presence of base and boronic acid;[18] (b) catalyst-derived transient intermediate; and (c) equilibrium of free and coordinated triphenylphosphine, as already found in the study of the oxidative addition (Fig. 2).

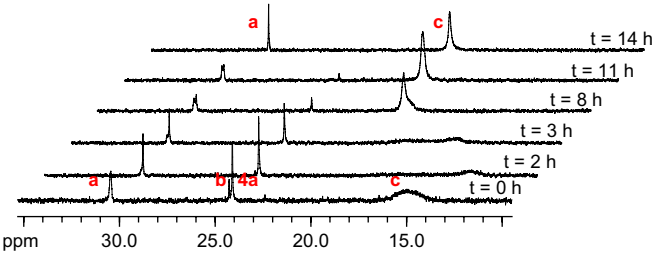

Figure 2. ^{31}P NMR study of the Suzuki–Miyaura reaction of pyridine **1a**, $PhB(OH)_2$, and $Pd(PPh_3)_4$. (a) Ph_3PO in the presence of base and boronic acid; (b) catalyst-derived transient intermediate; (c) equilibrium of L and 'PdL'.

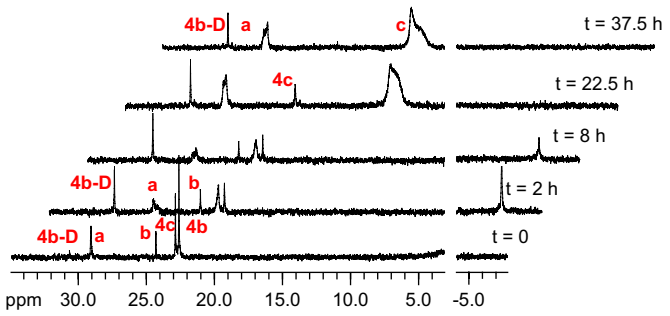

Figure 3. ^{31}P NMR study of the Suzuki–Miyaura reaction of pyridine **1b**, $PhB(OH)_2$, and $Pd(PPh_3)_4$. (a) Ph_3PO in the presence of base and boronic acid; (b) catalyst-derived transient intermediate; (c) equilibrium of L and 'PdL'.

On the other hand, for pyridine **1b**, similar to pyridine **1a**, the ^{31}P NMR displayed the signals previously assigned to Ph_3PO oxide (a), transient intermediate (b), and equilibrium of free and coordinated phosphine (c). However, in this case, another species, **4c** (^{31}P NMR, δ=22.74 ppm), appeared along with complexes **4b** and **4b-D** (Fig. 3).

Interestingly, the situation regarding the involved species was entirely the same when the starting materials of the transmetalation reactions were the corresponding isolated oxidative addition complexes, yet the transmetalation of the isolated complex **4a** was complete in 5 h.[19]

2.2. Computational study

The experimental NMR observation of an intermediate **4c** for transmetalation in the reaction of species **1b** is a novel and mechanistically relevant result. We decided to undertake a DFT study on the reaction with the double goal of characterizing **4c** and of understanding why it is present in the reaction of 2-bromo-4-phenylpyridine **1b** but not with other substrates. In previous works we had studied computationally the transmetalation process involving vinyl[9,20] and phenyl[21] groups as substrates to the cross-coupling reaction. Here we extend the study to bromophenylpyridine substrates. In particular, the reaction between the model system *trans*-[PdBr{C_5H_3N(4-C_6H_5)-C^2}(PH_3)$_2$] (**5**) and Ph-$B(OH)_3^-$ (**6**) is considered.

Figure 4 presents the energy profile corresponding to the reaction between **5** and **6**, and Figure 5 shows the optimized geometries of some of the structures. All computed structures are labeled as **I** or **TS** depending on their nature as intermediates or transition states, and those in this particular profile share the label **A**.

The overall reaction is similar to that observed in previous reports with other systems.[9,21] The transmetalation process begins with the initial approach between **5** and **6** and formation of the intermediate **IA1**. The reaction continues through the displacement of Br^- by the organoborate in the coordination sphere of the metal, which results in intermediate **IA2**, where the borate coordinates to the palladium through an oxygen atom. The rest of the process consists of the rearrangement of the borate Ph-$B(OH)_3^-$ group within the metal coordination sphere. First, the coordination to palladium shifts from the oxygen (in **IA2**) to the η^2 coordination of two carbon atoms of the phenyl group (in **IA3**). In the last step, the *ipso* carbon of the phenyl acquires an η^1 coordination to the metal, the C–B bond is broken, and the $B(OH)_3$ unit moves away from the metal (in **IA4**). The products, **7** and **8**, are obtained by the separation of the two fragments of **IA4**, in a slightly endothermic process (9.6 kcal/mol).

The energy profile in Figure 4 shows that the transmetalation step takes place quite smoothly for this system. The overall exothermicity is 14.9 kcal/mol. The highest energy transition state (**TSA3**) is 7.8 kcal/mol above the reactants and, more significantly, 24.7 kcal/mol above the lowest energy minimum (**IA1**). There are up to four different intermediates in the process (**IA1**, **IA2**, **IA3**, and **IA4**). However, not all of them are feasible candidates for the experimentally observed complex **4c**. The initial intermediate **IA1** is −16.9 kcal/mol below the reactants, and draws its stability from the fact that an anionic unit is approaching a metal center in gas phase. This large energy difference is mostly associated to the neglection of solvent and entropic effects in the current calculations, as has been shown in our previous studies on transmetalation.[9,21] This computational artifact affects critically only the energetics of bimolecular steps[20] like the one going from the separate reactants **5** and **6** to **IA1**. From a more chemical point of view, **IA1** is also a bad candidate for the experimentally observed intermediate, because it

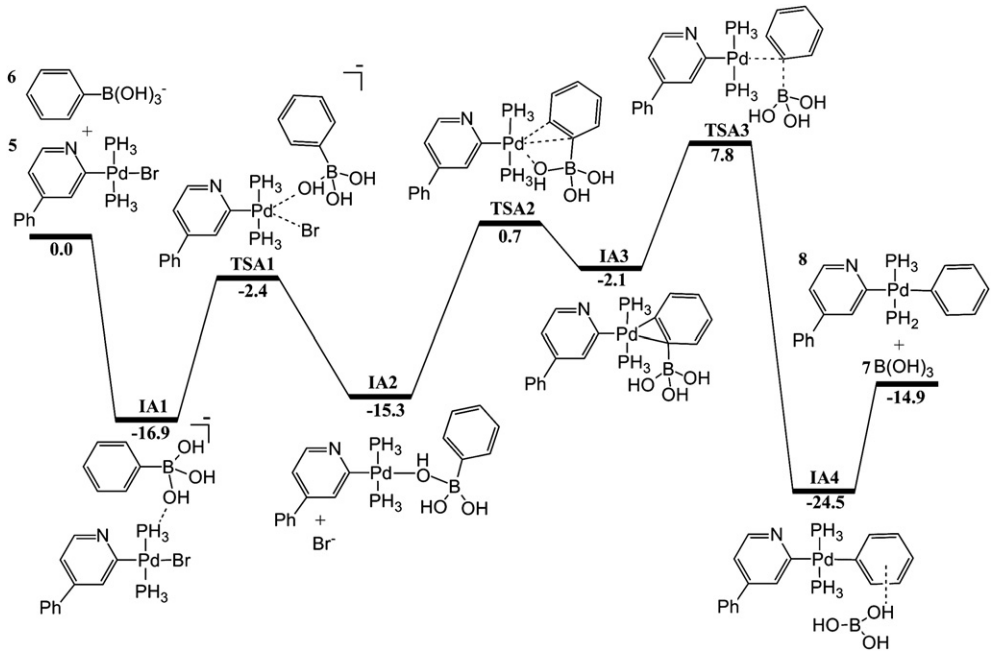

Figure 4. B3LYP energy profile for the transmetalation reaction between **5** and **6**. Relative energies are given in kcal/mol.

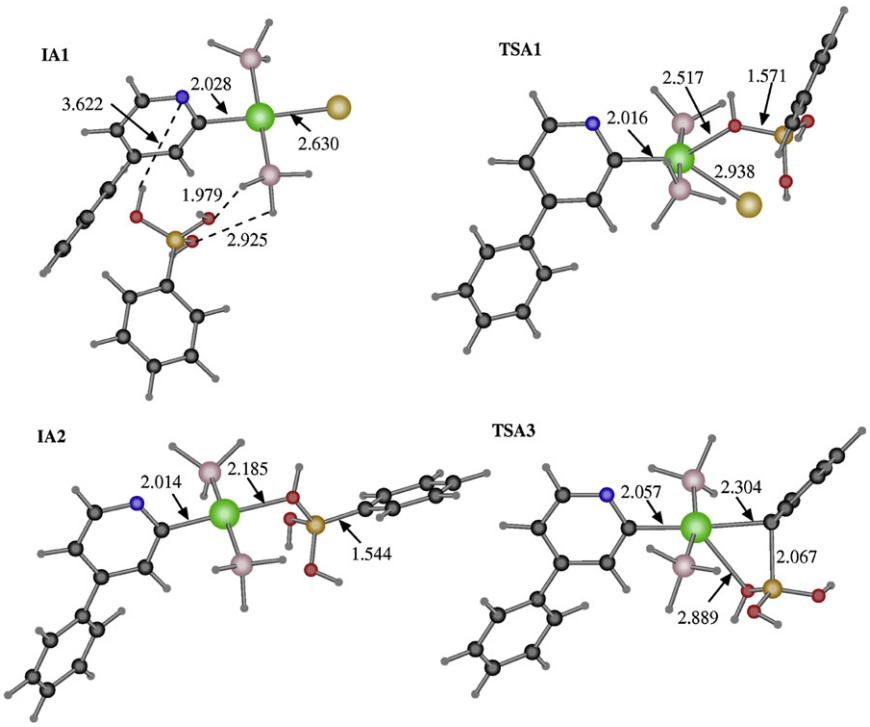

Figure 5. B3LYP structures for selected structures along the transmetalation reaction between **5** and **6**. Representative distances are given in Å.

does not present direct interactions between the two fragments that are likely to be affected by the nature of the bromophenylpyridine group. In fact, **IA1** must be better viewed as the computational model of the starting point of the transmetalation process. **IA4** must be discarded for similar reasons that **IA1**: the energetics of the uphill path from **IA4** to **7** plus **8** are likely overestimated, and this intermediate is the computational model for the final point of the transmetalation. Intermediate **IA3** is finally a bad candidate for a different reason. As can be seen in Figure 4, **IA3**, with a relative energy of −2.1 kcal/mol lies in a well between **TSA2** (energy of 0.7 kcal/mol) and **TSA3** (energy of 7.8 kcal/mol). The barrier for the backward reaction from **IA3** is only 2.8 kcal/mol, a value that will be easily overcome at room temperature, and makes thus unlikely the observation of this intermediate. This leaves **IA2** as the most likely candidate for the experimentally observed species **4c**. In order to confirm this hypothesis, we will analyze in what follows the energy profile corresponding to a system where the bromophenylpyridyl ligand is replaced by the more usual phenyl group.

Figures 6 and 7 present the energy profile and optimized geometries for the transmetalation step concerning *trans*-[PdBr{C_6H_5}(PH_3)$_2$], **9**, as model complex, and the same organoboronate anion **6**. Label **B** is used for structures in this profile to distinguish them from those previously discussed. There are small differences between the profile in Figure 6 and that in our previous work[21] because of minor changes in the computational method.

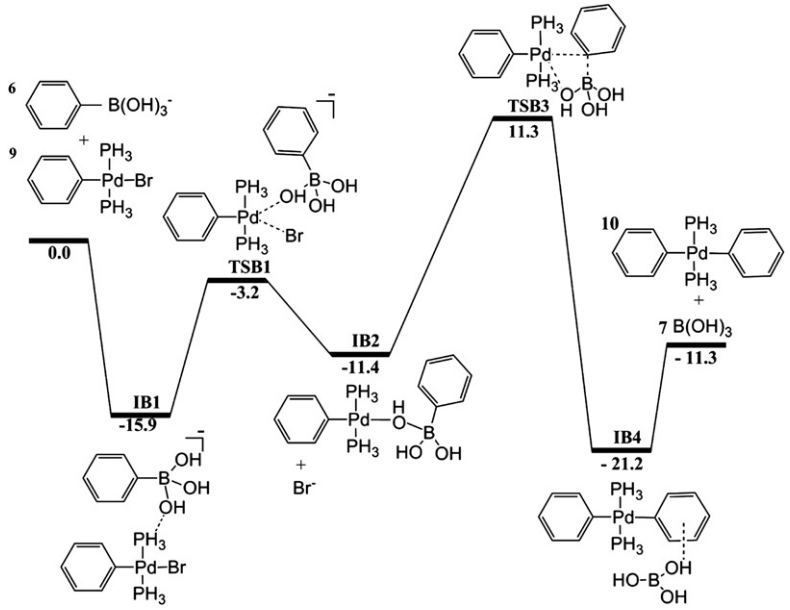

Figure 6. B3LYP energy profile for the transmetalation reaction between **6** and **9**. Relative energies are given in kcal/mol.

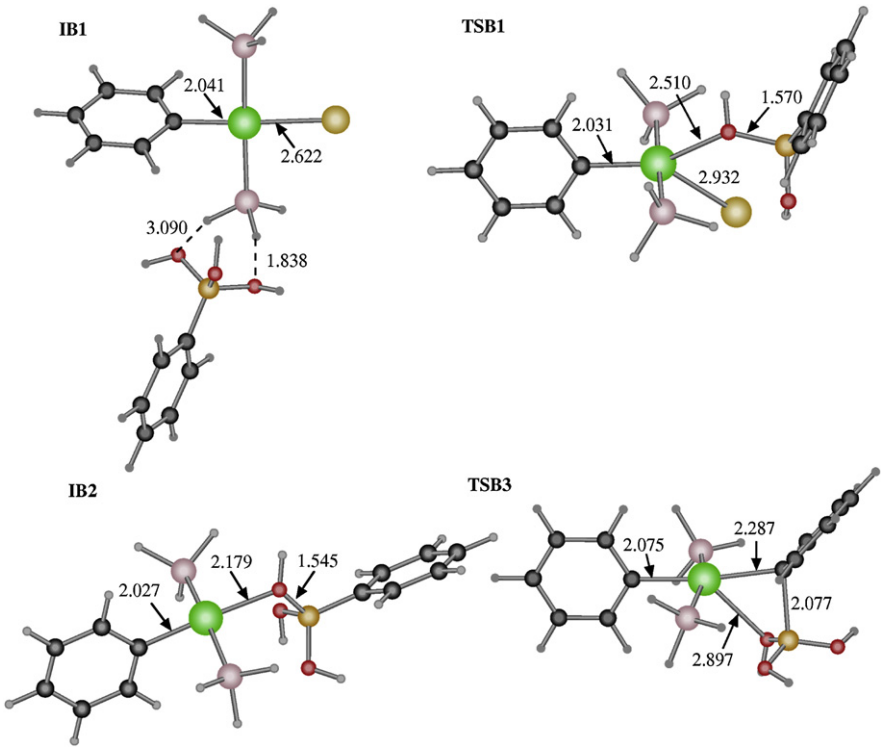

Figure 7. B3LYP structures for selected structures along the transmetalation reaction between **6** and **9**. Representative distances are given in Å.

The only qualitative difference between the profiles for bromophenylpyridyl (Fig. 4) and phenyl (Fig. 6) is the absence of intermediate **IB3** (and consequently of **TSB2**) in the latter. This is not critical, because intermediate **IA3** is already in a quite shallow well for the bromophenylpyridine system, as discussed above.

The overall energetics involved in transmetalation with the phenyl system are also smooth. The reaction is mildly exothermic, with the products −11.3 kcal/mol below the separated reactants. The kinetics are also reasonable for a room temperature process, the highest energy transition state (**TSB3**) is 27.2 kcal/mol above the lowest energy intermediate **IB1**. There is, however, a critical quantitative difference between the profiles in Figures 4 and 6, and it involves precisely the **IA1**/**IA2** and **IB1**/**IB2** pairs. In the case of the bromophenylpyridyl system, the intermediate **IA1** is 1.6 kcal/mol more stable than **IA2**. This energy difference is low enough to permit a sizeable presence of **IA2** in equilibrium with **IA1**. This fits perfectly with the presence of small concentrations of **4c** that has been experimentally monitored throughout the reaction. In the case of the phenyl system, the difference between the pair **IB1**/**IB2** has been calculated as 4.5 kcal/mol in favor of **IB1**. The larger energy difference involving **IB1**/**IB2** causes a strong displacement in the equilibrium towards **IB1** and consequently decreases the concentration of intermediate **IB2** below detection level. These results thus support our assignment of the computed intermediate **IA2** to the experimentally observed complex **4c**.

We can also analyze why this intermediate is observed for the particular case of the bromophenylpyridyl system, but not with phenyl or other more usual groups. The structures of **IA2** and **IB2** have been presented in Figures 5 and 7. It can be seen that they involve coordination of the organoboronate group to the metal through the oxygen atom of one of its hydroxyl groups. The interaction is quite strong, as proved by the Pd–O distances of 2.185 Å (**IA2**) and 2.179 Å (**IB2**). The distance is longer, thus indicative of a weaker coordination for **IA2**. This is consistent with a stronger trans influence of pyridyl, but may seem in contradiction with the fact that **IA2** is detectable, but **IB2** is not. The contradiction is solved by noticing that we are dealing with relative binding energies. The main contribution to the energy difference between **IA2** (**IB2**) and **IA1** (**IB1**) is not the absolute coordination energy of organoboronate, but its relative coordination energy with respect to bromide. Bromide is a better ligand than organoboronate, and the difference between the two ligands will decrease when their absolute coordination energy does.

An additional set of calculations on the reaction between *trans*-[PdBr{$C_5H_3N(4\text{-}C_6H_5)\text{-}C^4$}$(PH_3)_2$] (**11**) and Ph-$B(OH)_3^-$ (**6**) was carried out, and shown to produce results very similar to those of the phenyl system described above. The corresponding structures and energetics, provided in Supplementary data with labels **C**, indicate that the reported intermediate must be observable only for the case of 2-bromopyridine, but not for 4-bromopyridine, again in agreement with experiment.

The presence of neutral and negatively charged species on the overall reaction questioned the validity of the use of potential energies for the discussion of overall energetics. However, the approach is valid because the key comparisons are always carried out between species with the same charge. In any case, we confirmed the validity of this reasoning through an additional set of single-point calculations with the PCM method to account for the effects of a toluene solvent. The results are summarized in Table 1. The energy profiles obtained when the reaction takes place in gas phase or solution follow the same general patterns. For the reaction between **5** and **6**, with **A** labels, the overall barrier (difference between highest energy **TSA3** and lowest energy **IA1**) is 24.7 kcal/mol and the value is 22.7 kcal/mol in solution (difference between **TSA3** and **IA2**). The corresponding values for the reaction between **6** and **9** are 27.2 and 25.1 kcal/mol.

More critically to the topic under discussion, the energy differences between the **IB1**/**IB2** and **IA1**/**IA2** pairs follow the same trends. Intermediates **IA1** and **IA2** are much closer, with energy differences of 1.6 and −0.5 kcal/mol in gas phase and solution, respectively. This allows for **IA2** to be detected, and is thus the most likely candidate to be the experimentally observed species **4c**. In

Table 1
B3LYP energy profile (in kcal/mol) in gas phase and toluene solution for the transmetalation reaction between phenylboronate **6** and complexes **5** and **9**, respectively

	5+**6**		**6**+**9**	
	Gas phase	Solution	Gas phase	Solution
Reactants	0.0	0.0	0.0	0.0
I1	−16.9	−3.4	−15.9	−4.4
TS1	−2.4	7.6	−3.2	6.7
I2	−15.3	−3.9	−11.4	−1.6
TS2	0.7	11.2	—	—
I3	−2.1	8.8	—	—
TS3	7.8	18.7	11.3	20.7
I4	−24.5	−13.6	−21.2	−11.7
Product	−14.9	−8.5	−11.3	−6.5
I2–**I1**	1.6	−0.5	4.5	2.8

the case of the **IB1**/**IB2** pair, things are different, the energy differences are larger (4.5 and 2.8 kcal/mol, respectively), and this justifies that **IB2** is more difficult to monitor experimentally.

2.3. Conclusions

Our joint experimental and computational studies on the transmetalation step of the palladium-catalyzed Suzuki–Miyaura cross-coupling of bromophenylpyridines have allowed the characterization of a previously unreported intermediate, and this sheds further light in the understanding of the mechanism of this process. The experimental NMR evidences indicate the presence of an unknown species when the reaction is carried out and DFT calculations identify such intermediate as a *trans*-[Pd{Ph-B(OH)$_3^-$}{C_5H_2RN}(PR_3)$_2$] complex where the organoboronate anion coordinates the metal through the oxygen of one of its hydroxyl groups. The present experimental and theoretical results confirm the previous computational proposal that the transmetalation reaction takes place following a multistep mechanism where the organoboronic acid is initially activated by an external base, and attacks the palladium center as an organoboronate anion.

3. Experimental section

3.1. General

Reagents and solvents were purchased as reagent grade and used without further purification unless otherwise stated. Solvents were dried according to published methods[22] and distilled before use. All reactions were performed in oven-dried or flame-dried glassware under an inert atmosphere of Ar unless otherwise stated. NMR spectra were recorded in a Bruker AMX400 (400.13 and 100.61 MHz for proton and carbon, respectively) spectrometer at 298 K with residual solvent peaks as internal reference and the chemical shifts are reported in δ [parts per million], coupling constants J are given in hertz and the multiplicities expressed as follows: s=singlet, d=doublet, t=triplet, q=quartet, m=multiplet. Electronic impact ionization (EI) mass spectra were recorded on a VG-Autospec M instrument. Melting points (mp) were taken on a Stuart Scientific apparatus. Crystallographic data were collected on a Bruker Smart 1000 CCD diffractometer at CACTI (Universidade de Vigo) at 20 °C using graphite monochromated Mo Kα radiation (=0.71073 Å), and were corrected for Lorentz and polarization effects. The frames were integrated with the Bruker SAINT[23] software package and the data were corrected for absorption using the program SADABS.[24] The structures were solved by direct methods using the program SHELXS97.[25] All non-hydrogen atoms were refined with anisotropic thermal parameters by full-matrix least-squares calculations on F^2 using the program SHELXL97. Hydrogen atoms were inserted at calculated positions and constrained with isotropic thermal parameters. Drawings were produced with PLATON.[26]

3.1.1. *trans*-Bromo(2-phenylpyrid-4-yl-κC^4)bis(triphenylphosphane)palladium(II) (**4a**)

To a thoroughly degassed solution of $Pd(PPh_3)_4$ (0.15 g, 0.13 mmol) in toluene (1.0 mL), a solution of 4-bromo-2-phenylpyridine (**1a**) (31 mg, 0.13 mmol) in toluene (0.5 mL) was added dropwise. The reaction mixture was stirred at 50 °C for 18 h. Then, the solvent was removed under reduced pressure; the residue was titrated with ether yielding 83 mg (73%) of a solid, identified as complex **4a**. ^{1}H NMR (400 MHz, CD_2Cl_2) δ 6.75 (m, 1H, H^5), 6.99 (br s, 1H, H^3), 7.27–7.32 (m, 18H, H^6+Ph+PPh_3), 7.35–7.39 (m, 6H, PPh_3), 7.57–7.61 (m, 12H, PPh_3) ppm. ^{13}C NMR (100 MHz, CD_2Cl_2) δ 127.3 (CH), 128.2 (CH), 128.5 (CH), 128.5 (CH, virtual triplet, ^vJ=5.0 Hz), 130.8 (CH), 130.9 (CH), 131.4 (C, virtual triplet, ^vJ=23.3 Hz), 132.1 (CH, t), 135.2 (CH, virtual triplet, ^vJ=6.2 Hz), 141.2 (C), 146.1 (CH), 154.7 (C), 175.1 (C) ppm. ^{31}P NMR (162 MHz, CD_2Cl_2) δ 24.13 ppm. HRMS (ESI$^+$) calcd for $C_{47}H_{39}NP_2^{79}Br^{106}Pd$ 864.0771; found 864.0770.

3.1.2. *trans*-Bromo(4-phenylpyrid-2-yl-κC^2)bis(triphenylphosphane)palladium(II) (**4b**) and di-μ-(4-phenylpyrid-2-yl)-κN:κC^2-bis[bromotriphenylphosphanepalladium(II)] (**4b-D**)

To a thoroughly degassed solution of $Pd(PPh_3)_4$ (0.089 g, 0.08 mmol) in toluene (0.5 mL), a solution of 2-bromo-4-phenylpyridine (**1b**) (18 mg, 0.08 mmol) in toluene (0.5 mL) was added dropwise. The reaction mixture was stirred at 25 °C for 10 h. Then, the solvent was removed under reduced pressure; the residue was titrated with ether yielding 25 mg (30%) of complex **4b** along with complex **4b-D**. After crystallization from CH_2Cl_2/hexane, complex **4b-D** was obtained as a crystalline solid (mp >178 °C, decomp.). Data of mononuclear complex **4b**: ^{1}H NMR (400 MHz, CD_2Cl_2) δ 6.26 (dd, J=5.1, 1.8 Hz, 1H, H^5), 6.69 (d, J=1.8 Hz, 1H, H^3), 6.90–6.92 (m, 2H, Ph), 7.22–7.39 (m, 21H, Ph+PPh_3), 7.57–7.62 (m, 12H, PPh_3), 7.69 (d, J=5.1 Hz, 1H, H^6) ppm. ^{31}P NMR (162 MHz, CD_2Cl_2) δ 22.7 ppm.

Data of dimer **4b-D**: ^{1}H NMR (400 MHz, CD_2Cl_2) δ 6.81 (m, 2H, 2×H^5), 6.88 (m, 2H, 2×H^3), 7.08–7.10 (m, 4H, Ph), 7.25–7.32 (m, 18H, Ph+PPh_3), 7.37–7.40 (m, 6H, PPh_3), 7.84–7.89 (m, 12H, PPh_3), 8.60 (d, J=5.8 Hz, 1H, H^6), 8.61 (d, J=5.8 Hz, 1H, H^6) ppm. ^{13}C NMR (100 MHz, CD_2Cl_2) δ 117.7 (CH), 127.4 (CH), 128.8 (CH, d, $^3J_{C-P}$=10.9 Hz), 129.2 (CH), 129.3 (CH), 130.9 (CH), 131.8 (C, d, $^1J_{C-P}$=51.1 Hz), 135.5 (CH, d, $^2J_{C-P}$=11.6 Hz), 138.1 (C), 145.6 (C), 151.9 (CH), 186.6 (C) ppm. ^{31}P NMR (162 MHz, CD_2Cl_2) δ 30.22 ppm. HRMS (ESI$^+$) calcd for $C_{58}H_{47}N_2P_2^{79}Br_2^{108}Pd_2$ 1206.9684; found 1206.9654.

3.2. Crystal data and structural refinement for 4b-D

Crystallographic data were collected on a Bruker Smart 1000 CCD diffractometer at 20 °C using graphite monochromated Mo Kα radiation (λ=0.71073 Å), and were corrected for Lorentz and polarization effects. All non-hydrogen atoms were refined with anisotropic thermal parameters by full-matrix least-squares calculations on F^2 using the program SHELXL97. Hydrogen atoms were inserted at calculated positions and constrained with isotropic thermal parameters. The phenyl rings of triphenylphosphine ligands, with their hydrogen atoms included on stereochemical grounds, were refined anisotropically as rigid groups [C–C=distance=1.39 Å] except the C55–C60 ring whose carbon atoms having common anisotropic parameters. Reflection data were corrected for the diffuse scattering due to disordered dichloromethane molecules by means of the program SQUEEZE.[27] Empirical formula: $C_{58}H_{47}Br_2N_2P_2Pd_2$; formula weight: 1206.54; temperature: 293(2) K; crystal system: triclinic (P−1); unit cell dimensions: a=10.9508(12) Å, b=12.8812(14) Å, c=21.513(2) Å; α=72.632(2)°, β=83.787(3)°, γ=75.811(2)°; volume: 2805.9(5) Å^3; Z=2; density

(calculated): 1.428 Mg/m^3; absorption coefficient=2158 mm^{-1}. $F(000)$=1202; crystal size=0.44×0.37×0.06 mm^3; independent reflections 11,087 [R(int)=0.0486]; data/restraints/parameters=11,087/36/439; final R [$I>2\sigma(I)$]: R_1=0.0631, wR_2=0.1398; R indices (all data): R_1=0.1406, wR_2=0.1582.[28]

3.3. Computational details

All calculations have been performed with the Gaussian03 suite of programs.[29] Density functional theory (DFT) calculations were carried out using the B3LYP[30] functional. The basis set was LANL2DZ for Pd and Br,[31] and 6-31+G(d) for H, B, C, N, O, and P.[32] The basis set for Br was expanded to include polarization[33] and diffuse functions.[34] All energies presented are potential energies without solvation corrections. No symmetry constraints were imposed during structural optimizations. All stationary points were characterized through the number of negative Eigen values in their Hessian matrices.

Acknowledgements

We thank MEC, Spain (SAF2004-07131, CTQ2005-09000-C02-02/BQU), Xunta de Galicia, Generalitat de Catalunya and the ICIQ foundation for financial support and for an F.P.U. fellowship to C.S. and a Juan de la Cierva contract to A.A.C.B. We thank Dr. B. Cobelo for X-ray resolution.

Supplementary data

Crystallographic data for complex **4b-D**. Copy of ^1H and ^{13}C NMR spectra. Cartesian coordinates and absolute energies of all computed structures. Supplementary data associated with this article can be found in the online version, at doi:10.1016/j.tet.2008.05.018.

References and notes

1. (a) Li, J. J.; Gribble, G. W. *Palladium in Heterocyclic Chemistry*; Pergamon: Amsterdam, 2000, Chapter 4, pp 183–232; (b) Tagata, T.; Nishida, M. *J. Org. Chem.* **2003**, *68*, 9412–9415; (c) *Metal-Catalyzed Cross-Coupling Reactions*, 2nd ed.; De Meijere, A., Diederich, F., Eds.; Wiley-VCH: Weinheim, 2004.
2. (a) Hassan, J.; Sévignon, M.; Gozzi, C.; Schulz, E.; Lemaire, M. *Chem. Rev.* **2002**, *102*, 1359–1469.
3. (a) Miyaura, N.; Suzuki, A. *Chem. Rev.* **1995**, *95*, 2457–2483; (b) Miyaura, N. *J. Organomet. Chem.* **2002**, *653*, 54–57; (c) Suzuki, A. *J. Organomet. Chem.* **1999**, *576*, 147–168; (d) Bellina, F.; Carpita, A.; Rossi, R. *Synthesis* **2004**, 2419–2440; (e) Miyaura, N. *Metal-Catalyzed Cross-Coupling Reactions*, 2nd ed.; De Meijere, A., Diederich, F., Eds.; Wiley-VCH: Weinheim, 2004; Chapter 2, pp 41–124; (f) Suzuki, A. *Chem. Commun.* **2005**, 4759–4763.
4. (a) Nicolau, K. C.; Bulger, P. G.; Sarlah, D. *Angew. Chem., Int. Ed.* **2005**, *44*, 4442–4489; (b) Zeni, G.; Larock, R. C. *Chem. Rev.* **2006**, *106*, 4644–4680.
5. Matos, K.; Soderquist, J. A. *J. Org. Chem.* **1998**, *63*, 461–470.
6. (a) Casado, A. L.; Espinet, P. *Organometallics* **1998**, *17*, 954–959; (b) Goossen, L. J.; Koley, D.; Hermann, H.; Thiel, W. *Chem. Commun.* **2004**, 2141–2143; (c) Senn, H. M.; Ziegler, T. *Organometallics* **2004**, *23*, 2980–2988; (d) Zuidema, E.; van Leeuwen, P. W. N. M.; Bo, C. *Organometallics* **2005**, *24*, 3703–3710; (e) Ahlquist, M.; Norrby, P.-O. *Organometallics* **2007**, *26*, 550–553.
7. Review on transmetalation of arylpalladium and platinum complexes: Suzaki, Y.; Yagyu, T.; Psakada, K. *J. Organomet. Chem.* **2007**, *692*, 326–342.
8. (a) Barder, T. E.; Walker, S. D.; Martinelli, J. R.; Buchwald, S. L. *J. Am. Chem. Soc.* **2005**, *127*, 4685–4696; (b) Zhao, P. J.; Incarvito, C. D.; Hartwig, J. F. *J. Am. Chem. Soc.* **2007**, *129*, 1876–1877.
9. Braga, A. A. C.; Morgon, N. H.; Ujaque, G.; Maseras, F. *J. Am. Chem. Soc.* **2005**, *127*, 9298–9307.
10. (a) Goossen, L. J.; Koley, D.; Hermann, H. L.; Thiel, W. *J. Am. Chem. Soc.* **2005**, *127*, 11102–11114; (b) Nova, A.; Ujaque, G.; Maseras, F.; Lledós, A.; Espinet, P. *J. Am. Chem. Soc.* **2006**, *128*, 14571–14578; (c) Alvarez, R.; Faza, O. N.; de Lera, A. R.; Cárdenas, D. J. *Adv. Synth. Catal.* **2007**, *349*, 887–906; (d) Piechazyk, O.; Cantat, T.; Mezailles, N.; Le Floch, P. *J. Org. Chem.* **2007**, *72*, 4228–4237.
11. (a) Castedo, L.; Cid, M. M.; Seijas, J. A.; Villaverde, M. C. *Tetrahedron Lett.* **1991**, *32*, 3871–3872; (b) Sicre, C.; Cid, M. M. *Org. Lett.* **2005**, *7*, 5737–5739.
12. (a) Sicre, C.; Alonso-Gómez, J.-L.; Cid, M. M. *Tetrahedron* **2006**, *62*, 11063–11072; (b) For recent works on regioselectivity of palladium-catalyzed cross-couplings of heterocycles see: Fairlamb, I. J. *Chem. Soc. Rev.* **2007**, *36*, 1036–1045; (c) Schöter, S.; Stock, C.; Bach, T. *Tetrahedron* **2005**, *61*, 2245–2267; (d) Legault, C. Y.; Garcia, Y.; Merlic, C. A.; Houk, K. N. *J. Am. Chem. Soc.* **2007**, *129*, 12664–12665.
13. For isolated and characterized arylpalladium(II) complexes see: Fitton, P.; Rick, E. A. *J. Organomet. Chem.* **1971**, *28*, 287–291.
14. This low yield was attributed to difficulties encountered in the isolation procedure.
15. When this mixture was kept at 0 °C for 24 h, new species appeared (^{31}P NMR, δ = 31.00, 30.75, 30.35, and 22.20 ppm) that were assigned to bromine-bridged palladium complexes. The formation of these species seems to be reversible under the reactions conditions. (a) For other similar complexes see: Paul, F.; Patt, J.; Hartwig, J. F. *J. Am. Chem. Soc.* **1994**, *116*, 5969–5970; (b) Grushin, V. V.; Alper, H. *Organometallics* **1996**, *15*, 5242–5245.
16. See Figure 1 in Supporting data. For other related systems see: Ref. 12a and references therein.
17. Amatore, C.; Jutand, A.; M'Barki, M. A. *Organometallics* **1992**, *11*, 3009–3013.
18. For similar observations see: Mehta, P.; Zeldin, M. *Inorg. Chim. Acta* **1977**, *22*, L33–L34.
19. Although we observed only intermediates resulting from oxidative addition, the absence of signals corresponding to other intermediates does not prove that such intermediates are not involved. By means of ESI-MS more transient catalytic intermediates were observed in bromopyridines, see: Aliprantis, A. O.; Canary, J. W. *J. Am. Chem. Soc.* **1994**, *116*, 6985–6989.
20. Braga, A. A. C.; Ujaque, G.; Maseras, F. *Organometallics* **2006**, *25*, 3647–3658.
21. Braga, A. A. C.; Morgon, N. H.; Ujaque, G.; Lledós, A.; Maseras, F. *J. Organomet. Chem.* **2006**, *691*, 4459–4466.
22. Perrin, D.; Armarego, W. *Purification of Laboratory Chemicals*; Pergamon: Oxford, 1998.
23. *SMART (Control) and SAINT (Integration) Software*; Bruker Analytical X-ray Systems: Madison, WI, 1994.
24. Sheldrick, G. M. *SADABS. A Program for Absorption Corrections*; University of Göttingen: Germany, 1996.
25. Sheldrick, G. M. *SHELXS97. A Program for the Solution of Crystal Structures from X-ray Data*; University of Göttingen: Germany, 1997.
26. Spek, A. L. *PLATON. A Multipurpose Crystallographic Tool*; Utrecht University: Utrecht, The Netherlands, 2001.
27. van der Sluis, P.; Spek, A. L. *Acta Crystallogr., Sect.* **1990**, *A46*, 194–201.
28. Crystallographic data (excluding structure factors) for complex **4b–D** have been deposited with the Cambridge Crystallographic Data Center as supplementary publication no. CCDC 655939. Copies of the data can be obtained, free of charge, on application to CCDC, 12 Union Road, Cambridge CB2 1EZ, UK, (fax: +44-(0)1223-336033 or e-mail: deposit@ccdc.cam.ac.uk).
29. Frisch, M. J.; Trucks, G. W.; Schlegel, H. B.; Scuseria, G. E.; Robb, M. A.; Cheeseman, J. R.; Montgomery, J. A., Jr.; Vreven, T.; Kudin, K. N.; Burant, J. C.; Millam, J. M.; Iyengar, S. S.; Tomasi, J.; Barone, V.; Mennucci, B.; Cossi, M.; Scalmani, G.; Rega, N.; Petersson, G. A.; Nakatsuji, H.; Hada, M.; Ehara, M.; Toyota, K.; Fukuda, R.; Hasegawa, J.; Ishida, M.; Nakajima, T.; Honda, Y.; Kitao, O.; Nakai, H.; Klene, M.; Li, X.; Knox, J. E.; Hratchian, H. P.; Cross, J. B.; Bakken, V.; Adamo, C.; Jaramillo, J.; Gomperts, R.; Stratmann, R. E.; Yazyev, O.; Austin, A. J.; Cammi, R.; Pomelli, C.; Ochterski, J. W.; Ayala, P. Y.; Morokuma, K.; Voth, G. A.; Salvador, P.; Dannenberg, J. J.; Zakrzewski, V. G.; Dapprich, S.; Daniels, A. D.; Strain, M. C.; Farkas, O.; Malick, D. K.; Rabuck, A. D.; Raghavachari, K.; Foresman, J. B.; Ortiz, J. V.; Cui, Q.; Baboul, A. G.; Clifford, S.; Cioslowski, J.; Stefanov, B. B.; Liu, G.; Liashenko, A.; Piskorz, P.; Komaromi, I.; Martin, R. L.; Fox, D. J.; Keith, T.; Al-Laham, M. A.; Peng, C. Y.; Nanayakkara, A.; Challacombe, M.; Gill, P. M. W.; Johnson, B.; Chen, W.; Wong, M. W.; Gonzalez, C.; Pople, J. A. *Gaussian 03, Revision C.02*; Gaussian: Wallingford, CT, 2004.
30. (a) Lee, C.; Parr, R. G.; Yang, W. *Phys. Rev.* **1988**, *37*, 785–789; (b) Becke, A. D. *J. Phys. Chem.* **1993**, *98*, 5648–5652; (c) Stephens, P. J.; Devlin, F. J.; Chabalowski, C. F.; Frisch, M. J. *J. Chem. Phys.* **1994**, *98*, 11623–11627.
31. (a) Hay, P. J.; Wadt, W. R. *J. Chem. Phys.* **1985**, *82*, 299–310; (b) Wadt, W. R.; Hay, P. J. *J. Chem. Phys.* **1985**, *82*, 284–298.
32. (a) Francl, M. M.; Pietro, W. J.; Hehre, W. J.; Binkley, J. S.; Gordon, M. S.; Defrees, D. J.; Pople, J. A. *J. Chem. Phys.* **1982**, *77*, 3654–3665; (b) Clark, T.; Chandrasekhar, J.; Spitznagel, G. W.; Schleyer, P. V. *J. Comput. Chem.* **1983**, *4*, 294–301.
33. Höllwarth, A.; Böhme, M.; Dapprich, S.; Ehlers, A. W.; Gobbi, A.; Jonas, V.; Köhler, K. F.; Stegmann, R.; Veldkamp, A.; Frenking, G. *Chem. Phys. Lett.* **1993**, *208*, 237–240.
34. Check, C. E.; Faust, T. O.; Bailey, J. M.; Wright, B. J.; Gilbert, T. M.; Sunderlin, L. S. *J. Phys. Chem. A* **2001**, *105*, 8111–8116.